Supporting Information

Functional Carbon Quantum Dots for Highly Sensitive Graphene Transistors for Cu^{2+} Ion Detection

Qin Fan,† Jinhua Li,*,† Yuhua Zhu,† Zilu Yang,† Tao Shen,† Yizhong Guo,‡ Lihua Wang,‡ Tao Mei,† Jianying Wang,*,† Xianbao Wang†

†Hubei Collaborative Innovation Center for Advanced Organic Chemical Materials, Key Laboratory for the Green Preparation and Application of Functional Materials, Ministry of Education, Hubei Key Laboratory of Polymer Materials, School of Materials Science and Engineering, Hubei University, Wuhan 430062, China

‡Institute of Microstructure and Properties of Advanced Materials, Beijing University of Technology, Beijing 100124, China

Corresponding Author

*Email: jinhua_li@hubu.edu.cn (J.L.); wangjy_2002@163.com (J.W.).

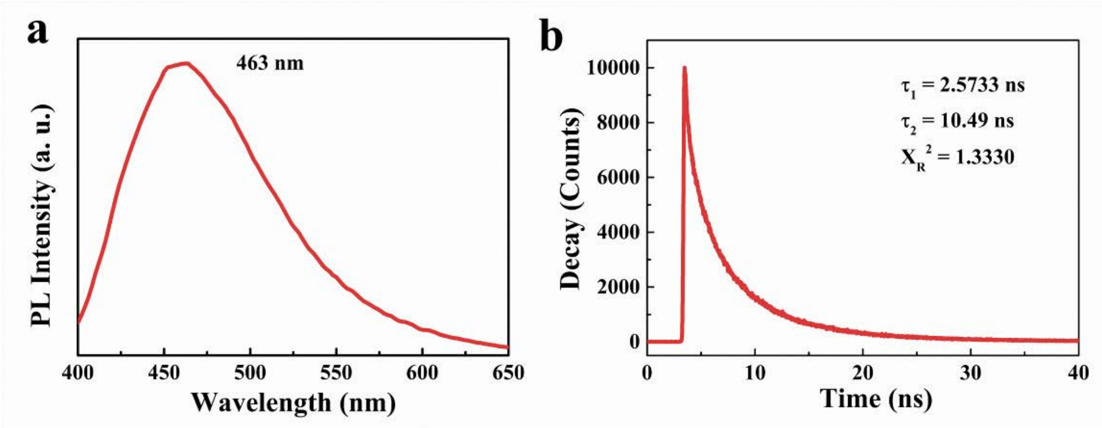

Figure S1. (a) The PL spectrum of CQDs. (b) The luminescence decay profile of CQDs.

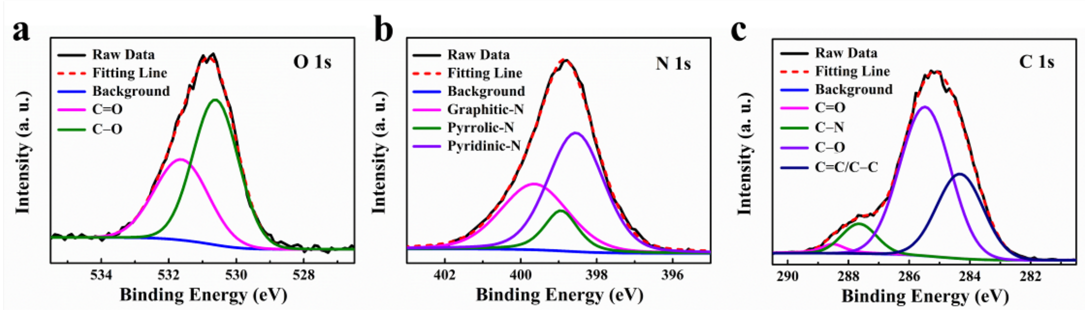

Figure S2. (a) High-resolution O1s XPS spectrum of CQDs. (b) High-resolution N1s XPS spectrum of CQDs. (c) High-resolution C1s XPS spectrum of CQDs.

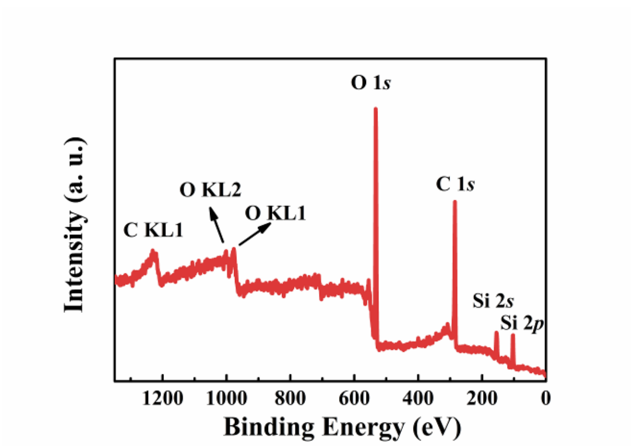

Figure S3. XPS spectrum of the graphene film on the SiO_2 substrate.

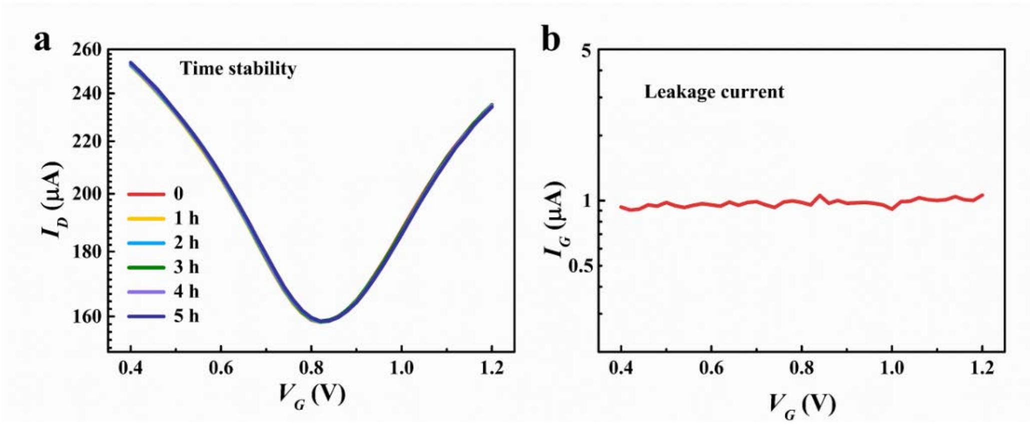

Figure S4. (a) Time stability of CQDs functional SGGT. (b) Leakage current of CQDs functional SGGT.

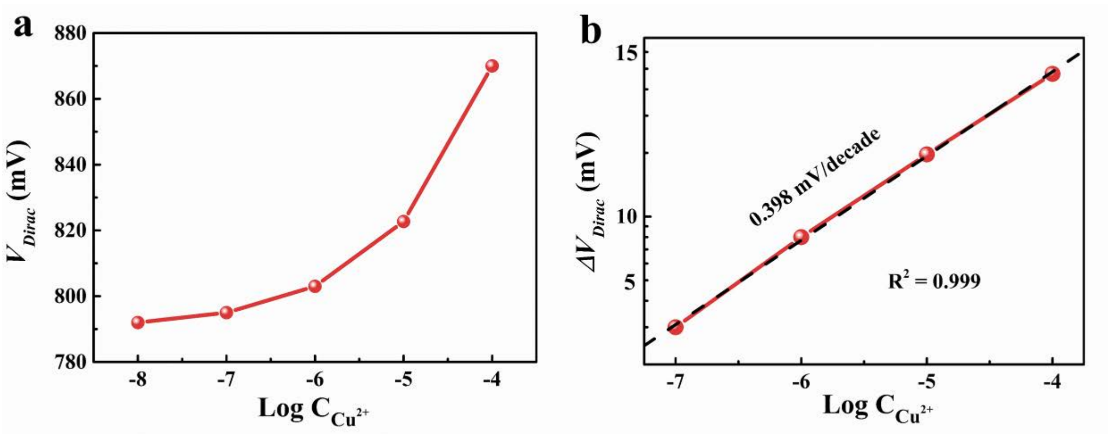

Figure S5. (a) The Dirac voltage (V_{Dirac}) of CQDs functional SGGT versus the logarithmic value of Cu^{2+} ion concentration. (b) The Dirac voltage change (ΔV_{Dirac}) of CQDs functional SGGT versus the logarithmic value of Cu^{2+} ion concentration.

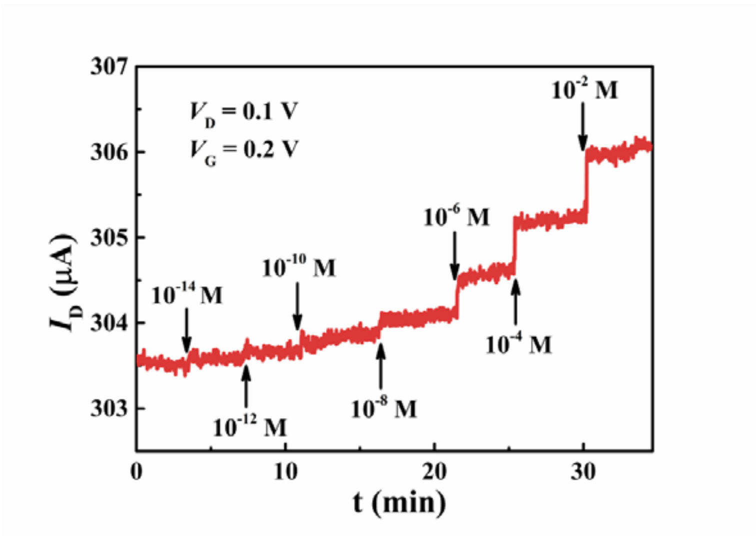

Figure S6. Channel current responses of CQDs functional SGGT to the increasing Cu^{2+} ion concentration in PBS solution measured at V_D = 0.01 V and V_G = 0.2 V.

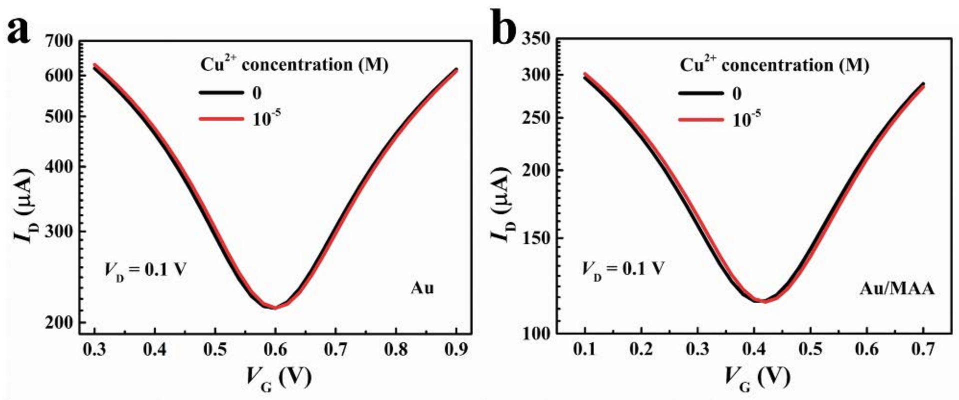

Figure S7. (a) Transfer curve of SGGT with the gate of Au before and after Cu^{2+} ions. (b) Transfer curve of SGGT with the gate of Au/MAA before and after Cu^{2+} ions.

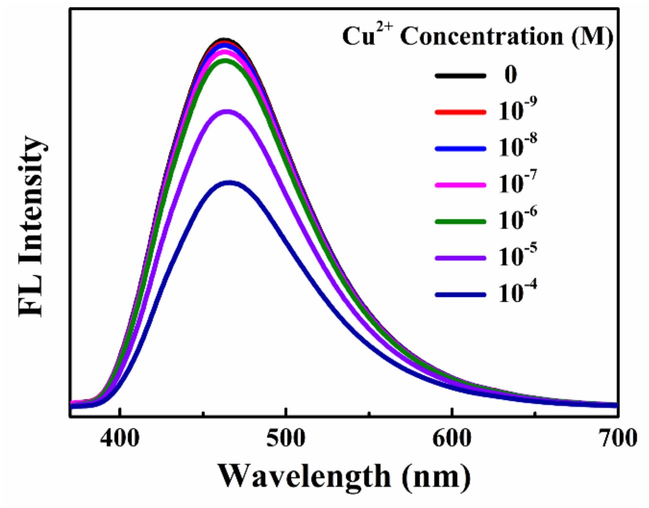

Figure S8. FL spectra of CQDs upon the addition of various concentrations of Cu^{2+} ions.

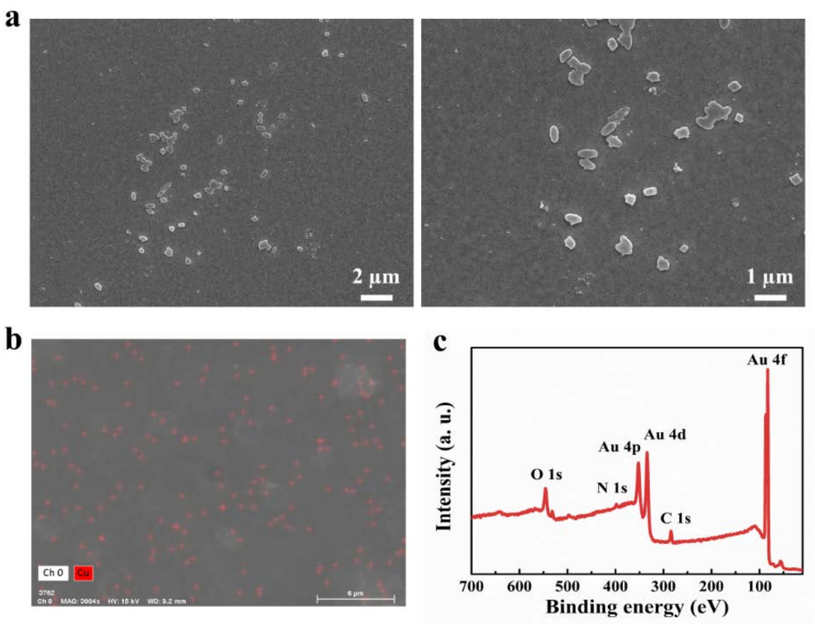

Figure S9. Characterization of the gate surface after detection. (a) SEM image of the gate electrodes after detecting Cu^{2+} ions. (b) Element mapping result of the gate electrodes after detecting Cu^{2+} ions. (c) Full range XPS survey spectrum of the gate electrodes.

Table S1. Comparison on recently reported various methods for detection of Cu^{2+} ions.

Detection Method	Materials	LOD	Linear Range	Ref.
Electrochemiluminescence	$CoFe_2O_4$ MNPs	0.1 pM	0.1 pM – 0.1 μM	1
Electrochemistry	PSC@Au-DNAzyme	0.33 pM	1 pM – 0.5 μM	2
EGOFET	GGH	1 pM	1 pM – 10 nM	3
Electrochemistry	Au/Me_2NH_2@MOF-1/GCE	1 pM	5 pM – 0.9 μM	4
Fluorescence	MNPs@Cu-Sub@Cu-Enzy	1 pM	10 pM – 0.2 μM	5
Fluorescence	g-C_3N_4	8 pM	10 pM – 0.4 nM	6
Electrochemistry	HRP-Cu-Gly	42.4 pM	0.5 nM – 30 nM	7
Fluorescence	Au@SiO_2-CDs	80 pM	0.1 nM – 0.1 μM	8
Colorimetry	His-AuNCs	0.1 nM	1 nM – 0.1 μM	9
Fluorescence	$CsPbBr_3$	0.1 nM	0 – 0.1 μM	10
Colorimetry	GSH-AuNCs	0.125 nM	0.125 nM – 0.125 mM	11
Fluorescence	UCNP	0.16 nM	0.4 – 40 nM	12
SERS	MarR	0.18 nM	0.5 nM − 1 μM	13
Fluorescence	QDs-Abs	0.2 nM	1 nM – 0.8 μM	14
Fluorescence	DTBL	0.32 nM	0 – 3.4 μM	15
Fluorescence	MPA-CdTe QDs	0.36 nM	0 – 0.1 μM	16
Fluorescence	QG-scaffolded COFs	0.5 nM	1 nM – 10 μM	17
Fluorescence	OS-g-C_3N_4-dots	0.7 nM	3 nM – 10 μM	18
Fluorescence	Schiff base	0.73 nM	–	19
Chemiluminescence	gold nanostar	0.9 nM	2 nM – 9 μM	20
Electrochemistry	PAAM/PA/PDA	1 nM	1 nM – 1 μM	21
Fluorescence	bCDs/gQDs/rQDs	1.3 nM	–	22
SGGT	CQDs	10 fM	10 fM – 0.1 nM, 0.1 nM – 0.1 mM	This work

Abbreviations: LOD, limit of detection; MNPs, magnetite nanoparticles; PSC, polystyrene microsphere; EGOFET, electrolyte-gated organic field-effect transistor; GGH, glycine-glycine-histidine; MOF, metal organic Frameworks; GCE, glassy carbon electrode; Sub, cleavage substrate sequence; Enzy, consists of a catalytic sequence; HRP, horse radish peroxidase; Gly, glycine; CDs, carbon dots; NCs, nanoclusters; GSH, glutathione; UCNP, upconversion nanoparticle; SERS, surfaceenhanced Raman scattering; MarR, multiple antibiotic resistance regulator; QDs-Abs, antibodies functionalized quantum dots; DTBL, A novel p-dimethylaminobenzamide-based Schiff base derivative; MPA, 3-mercaptopropionic acid; QDs, quantum dots; QG, quaternized graphene; COF, covalent organic frameworks; OS-g-C_3N_4-dots, the oxygen and sulfur co-doped graphitic carbon nitride quantum dots; PMMA, polyacrylamide; PA, phytic acid; PDA, polydopamine; bCDs, blue-emission carbon dots; gQDs, green-emission quantum dots; rQDs, red-emission quantum dots; SGGT, solution-gated graphene transistor.

Table S2. Summary of solution-gated transistors for Cu^{2+} ion detection.

LOD	Active Layer	Ref.
10 μM	*p*-tert-butylcalix [9 and 11] arene	23
2.5 μM	Polycarbazole	24
1 nM	*n*-Si	25
96 ppb	PBTTT	26
100 nM	PEDOT:PSS	27
10 nM	rGO	28
1 pM	DPP-DTT	3
0.01 pM	Si-nanoribbon	29
10 fM	CVD graphene	This work

Abbreviations: LOD, limit of detection; PBTTT, poly{2,5-bis(3-hexadecylthiophene-2-yl)-thieno[3,2-b]thiophene}; PEDOT:PSS, poly(3,4-ethylenedioxythiophene) polystyrene sulfonate; DPP-DTT, poly{2,5-(2-octyldodecyl)-3,6-diketopyrrolopyrrole-alt-5,5-(2,5-di(thien-2-yl)thieno[3,2-b]thiophene)}.

REFERENCES

(1) Lei, Y. M.; Xiao, B. Q.; Liang, W. B.; Chai, Y. Q.; Yuan, R.; Zhuo, Y. A Robust, Magnetic, and Self-Accelerated Electrochemiluminescent Nanosensor for Ultrasensitive Detection of Copper Ion. *Biosens. Bioelectron.* **2018**, *109*, 109–115.

(2) Qing, M.; Xie, S.; Cai, W.; Tang, D.; Tang, Y.; Zhang, J.; Yuan, R. Click Chemistry Reaction-Triggered 3D DNA Walking Machine for Sensitive Electrochemical Detection of Copper Ion. *Anal. Chem.* **2018**, *90* (19), 11439–11445.

(3) Nguyen, T. T. K.; Tran, H. V.; Vu, T. T.; Reisberg, S.; Noel, V.; Mattana, G.; Pham, M. C.; Piro, B. Peptide-Modified Electrolyte-Gated Organic Field Effect Transistor. Application to Cu^{2+} Detection. *Biosens. Bioelectron.* **2019**, *127*, 118–125.

(4) Jin, J. C.; Wu, J.; Yang, G. P.; Wu, Y. L.; Wang, Y. Y. A Microporous Anionic Metal-Organic Framework for a Highly Selective and Sensitive Electrochemical Sensor of Cu^{2+} Ions. *Chem. Commun.* **2016**, *52* (54), 8475–8478.

(5) Xiong, Y.; Meng, P.; Li, H.; Hu, Y.; Zhou, L.; Jiang, S.; Pang, Y.; Li, S.; Huang, P. Dual Signal Amplification Strategy for High-Sensitivity Detection of Copper Species in Bio-Samples with a Tunable Dynamic Range. *Chem. Commun.* **2018**, *54* (20), 2542–2545.

(6) Guo, X.; Wang, Y.; Wu, F.; Ni, Y.; Kokot, S. Preparation of Protonated, Two-Dimensional Graphitic Carbon Nitride Nanosheets by Exfoliation, and their Application as a Fluorescent Probe for Trace Analysis of Copper(II). *Microchim. Acta* **2015**, *183* (2), 773–780.

(7) Li, J.; Zhang, L.; Wei, G.; Zhang, Y.; Zeng, Y. Highly Sensitive and Doubly Orientated Selective Molecularly Imprinted Electrochemical Sensor for Cu^{2+}. *Biosens. Bioelectron.* **2015**, *69*, 316–320.

(8) Zhou, Y.; Ma, Z. A Novel Fluorescence Enhanced Route to Detect Copper(II) by Click Chemistry-Catalyzed Connection of Au@SiO_2 and Carbon Dots. *Sens. Actuators B* **2016**, *233*, 426–430.

(9) Liu, Y.; Ding, D.; Zhen, Y.; Guo, R. Amino Acid-Mediated “Turn-Off/Turn-On” Nnanozyme Activity of Gold Nanoclusters for Sensitive and Selective Detection of Copper Ions and Histidine. *Biosens. Bioelectron.* **2017**, *92*, 140–146.

(10) Liu, Y.; Tang, X.; Zhu, T.; Deng, M.; Ikechukwu, I. P.; Huang, W.; Yin, G.; Bai, Y.; Qu, D.; Huang, X.; Qiu, F. All-Inorganic $CsPbBr_3$ Perovskite Quantum Dots as a Photoluminescent Probe for Ultrasensitive Cu^{2+} Detection. *J. Mater. Chem. C* **2018**, *6* (17), 4793–4799.

(11) Zhao, Q.; Yan, H.; Liu, P.; Yao, Y.; Wu, Y.; Zhang, J.; Li, H.; Gong, X.; Chang, J. An Ultra-Sensitive and Colorimetric Sensor for Copper and Iron Based on Glutathione-Functionalized Gold Nanoclusters. *Anal. Chim. Acta* **2016**, *948,* 73–79.

(12) Chen, H.; He, K.; Li, H.; Zhang, Y.; Yao, S. Analyte-Triggered Cyclic Autocatalytic Oxidation Amplification Combined with an Upconversion Nanoparticle Probe for Fluorometric Detection of Copper(II). *Microchim. Acta* **2018**, *185* (10), 484–492.

(13) Wang, Y.; Su, Z.; Wang, L.; Dong, J.; Xue, J.; Yu, J.; Wang, Y.; Hua, X.; Wang, M.; Zhang, C.; Liu, F. SERS Assay for Copper(II) Ions Based on Dual Hot-Spot Model Coupling with MarR Protein: New Cu^{2+}-Specific Biorecognition Element. *Anal. Chem.* **2017**, *89* (12), 6392–6398.

(14) Xiong, Y.; Zhou, L.; Wang, H.; Li, H.; Hu, Y.; Meng, P.; Zhang, X.; Huang, P. Rapid Laboratory Diagnosis of Wilson's Disease: One-Step Simultaneous Detection of Exchangeable Copper and Ceruloplasmin in Serum Based on Nanotechnology. *Sens. Actuators B* **2019**, *281*, 713–719.

(15) Xiong, J.-J.; Huang, P.-C.; Zhou, X.; Wu, F.-Y. A Highly Selective and Sensitive “Turn-On” Fluorescent Probe of Cu^{2+} by p-Dimethylaminobenzamide-Based Derivative and its Bioimaging in Living Cells. *Sens. Actuators B* **2016**, *232*, 673–679.

(16) Wang, Y.; Zhang, C.; Chen, X.; Yang, B.; Yang, L.; Jiang, C.; Zhang, Z. Ratiometric Fluorescent Paper Sensor Utilizing Hybrid Carbon Dots-Quantum Dots for the Visual Determination of Copper Ions. *Nanoscale* **2016**, *8* (11), 5977–5984.

(17) Cai, Y.; Jiang, Y.; Feng, L.; Hua, Y.; Liu, H.; Fan, C.; Yin, M.; Li, S.; Lv, X.; Wang, H. Q-Graphene-Scaffolded Covalent Organic Frameworks as Fluorescent Probes and Sorbents for the Fluorimetry and Removal of Copper Ions. *Anal. Chim. Acta* **2019**, *1057*, 88–97.

(18) Wang, H.; Lu, Q.; Li, M.; Li, H.; Liu, Y.; Li, H.; Zhang, Y.; Yao, S. Electrochemically Prepared Oxygen and Sulfur Co-Doped Graphitic Carbon Nitride Quantum Dots for Fluorescence Determination of Copper and Silver Ions and Biothiols. *Anal. Chim. Acta* **2018**, *1027*, 121–129.

(19) Chandra, R.; Ghorai, A.; Patra, G. K. A Simple Benzildihydrazone Derived Colorimetric and Fluorescent “*On-Off-On*” Sensor for Sequential Detection of Copper (II) and Cyanide Ions in Aqueous Solution. *Sens. Actuators B* **2018**, *255*, 701–711.

(20) Amjadi, M.; Abolghasemi-Fakhri, Z. Gold Nanostar-Enhanced Chemiluminescence Probe for Highly Sensitive Detection of Cu (II) Ions. *Sens. Actuators B* **2018**, *257*, 629–634.

(21) Zhao, Z.; Chen, H.; Zhang, H.; Ma, L.; Wang, Z. Polyacrylamide-Phytic Acid-Polydopamine Conducting Porous Hydrogel for Rapid Detection and Removal of Copper (II) Ions. *Biosens. Bioelectron.* **2017**, *91*, 306–312.

(22) Cai, Y.; You, J.; You, Z.; Dong, F.; Du, S.; Zhang, L. Profuse Color-Evolution-Based Fluorescent Test Paper Sensor for Rapid and Visual Monitoring of Endogenous Cu^{2+} in Human Urine. *Biosens. Bioelectron.* **2018**, *99*, 332–337.

(23) Mlika, R.; Dumazet, I.; Ouada, H. B.; Jaffrezic-Renault, N.; Lamartine, R.; Gamoudi, M.; Guillaud, G. Cu^{2+}-ISFET Type Microsensors Based on Thermally Evaporated *p*-Tert-Butylcalix [9 and 11] Arene Thin Films. *Sens. Actuators, B* **2000**, *62* (1), 8–12.

(24) Saxena V, Shirodkar V, Prakash R. Copper (II) Ion-Selective Microelectrochemical Transistor. *J. Solid State Electrochem.* **2000**, *4* (4), 234–236.

(25) Wustoni, S.; Hideshima, S.; Kuroiwa, S.; Nakanishi, T.; Mori, Y.; Osaka, T. Label-Free Detection of Cu (II) in a Human Serum Sample by Using a Prion Protein-Immobilized FET Sensor. *Analyst* **2015**, *140* (19), 6485–6488.

(26) Sasaki, Y.; Minami, T.; Minamiki, T.; Tokito, S. An Organic Transistor-Based Electrical Assay for Copper (II) in Water. *Electrochemistry* **2017**, *85* (12), 775–778.

(27) Xiong, C.; Qu, H.; Chen, W.; Zhang, L.; Qiu, L.; Zheng, L.; Xia, F. Real-Time Detection of Cu (II) with PEDOT: PSS Based Organic Electrochemical Transistors. *Sci. China: Chem.* **2017**, *60* (9), 1205–1211.

(28) Piccinini, E.; Bliem, C.; Reiner-Rozman, C.; Battaglini, F.; Azzaroni, O.; Knoll, W. Enzyme-Polyelectrolyte Multilayer Assemblies on Reduced Graphene Oxide Field-Effect Transistors for Biosensing Applications. *Biosens. Bioelectron.* **2017**, *92*, 661–667.

(29) Synhaivska, O.; Mermoud, Y.; Baghernejad, M.; Alshanski, I.; Hurevich, M.; Yitzchaik, S.; Wipf, M.; Calame, M. Detection of Cu^{2+} Ions with GGH Peptide Realized with Si-Nanoribbon ISFET. *Sensors* **2019**, *19* (18), 4022.